CAD Based Mechanistic Modeling of Forces for Generic Drill Point Geometry

K. Sambhav[1], S. G. Dhande[2] and P. Tandon[3]

[1]Indian Institute of Technology Kanpur, sambhav@iitk.ac.in
[2]Indian Institute of Technology Kanpur, sgd@iitk.ac.in
[3]PDPM Indian Institute of Information Technology, ptandon@iiitdm.in

ABSTRACT

The paper presents a methodology to model the geometry and forces of twist drills with generic point geometry. Starting from a detailed computer-aided designed (CAD) geometric model for a fluted twist drill in terms of bi-parametric surface patches using NURBS to present a generic model for the cutting lip and chisel edge, mechanistic model has been used to predict the forces. Optimization technique has been employed to obtain the points of intersection of surface patches. Using mechanistic model for normal and friction forces for the oblique cutting elements on the cutting lips and the chisel edge, the force components have been calculated, resolved and integrated to give the total thrust and torque for the generic profile of the drill.

Keywords: generic drill point geometry, NURBS, mechanistic modeling.
DOI: 10.3722//cadaps.2010.809-819

1 INTRODUCTION

1.1 Geometric Modeling

Drill point geometry has a significant effect on the drill performance and is the most critical portion of the drill [19]. It is uniquely determined by the configurations of the drill flank and the flute. Galloway [11] developed a conical grinding principle for the conventional point geometry, which was used by Fujii et al. [9-10] to develop a drill flank contour program to analyze the geometry using computers. The investigation used a conical drill with straight cutting edges only and the drill margin was not considered in the analysis. Armarego and Cheng [1] analyzed only the cylindrical flank configuration which resulted in the tool clearance angle being constant from the chisel edge to the outer edge, though it is required that the clearance angle should be greater near chisel edge. Fugelso [6-7] tried to solve this problem in cylindrical grinding by rotating the drill about its own axis with a slight penalty of having a slightly curved edge near the chisel edge. This altered the relationship between the clearance angle and the radius. Tsai and Wu [19] attempted to develop a comprehensive mathematical model for conical, hyperboloidal and ellipsoidal drills, but the model of an arbitrary geometry was not given. Stephenson and Agapiou [17] presented a parametric description of complex point geometries but they were not related to the grinding parameters. Chandrashekharan et al. [3-4] measured points on the cutting lip of the drill and fitted polynomial equations to determine the parametric form of the

edge. Here again, the geometry was not related to the grinding parameters. Paul et al. [13-14] optimized the shape of the point of the drill for minimum thrust and torque using grinding parameters which in turn were based on the conical and quadratic grinding surfaces. They first modeled the cutting lip and chisel edge in a discretized form and used them to obtain the oblique cutting angles.

Lin et al. [12] developed a mathematical model for a helical drill point geometry, specifically intended for micro-drills and showed that the model was more general than the commonly used conical, cylindrical and planar drill point models which were only special cases of this model. Theyalso obtained curved (convex or concave) cutting lip shapes for different semi-point angles using helical grinding. Galloway [11] and Fugelso [6, 7] have also stressed that curved cutting lip shapes result in a longer drill life than a straight lip for various working conditions and working materials. Shi et al. [16] conducted a study on curved edge drills and optimized the cutting edge shape to realize a desired rake angle distribution. Xiong et al. [22] developed a new methodology for designing a curve-edged twist drill with an arbitrarily given distribution of the cutting angles along the cutting edges.

Tandon et al. [18] represented the sectional view of the drill to be made up of arcs and straight lines and presented a model of conical grinding in terms of 3D angles. They established relations between conventional 2D angles and rotational 3D angles and gave a mapping guide to go from 2D to 3D angles and vice-versa. This helped evolve a new CAGD based 3D nomenclature for geometric definition of the drill.

A generalized approach to directly represent the sectional profile of the drill and the grinding profiles using NURBS has not been reported in the literature at yet. If the section of the drill and the generatrix of grinder can be given a generic shape, freedom to develop optimum geometry of a drill can be made available. In this paper, the sectional profile and the grinding profile have been represented by NURBS to give the generic geometric model of the drill. The cutting lips and the chisel edge have been obtained by finding the surface-surface intersection points using optimization algorithms [5] (reducing the problem to surface-curve intersections).

1.2 Force Modeling

Force modeling for a twist drill has been mostly done for conical grinding profiles [1-2], [15], [20], [21]. Stephenson and Agapiou [17] modeled the forces for drills with arbitrary cutting edges for the first time. Fuh and Chen [8] modeled the forces for curved primary cutting edges and showed that the thrust and torque can be significantly reduced with curved edges owing to the fact that it improves the distribution of the tool orthogonal rake angles along the primary cutting edge. Chandrashekharan et al. [3-4] gave a detailed mechanistic approach to model the forces which was used by Paul et al. [13-14] to optimize the drill point geometry. Still, a generalized approach to model the forces for a generic profile based on grinding parameters is yet to be presented.

2 GEOMETRIC MODELLING OF DRILL

Drills are rotary cutting tools used for the generation of holes. They have two or more cutting lips and flutes. The flutes allow for the passage of chips and cutting fluids. Drills are widely classified on the basis of their type, shank configuration, length, helix angle, number of flutes, hand of cut and drill profiles. The most common drills are helically fluted twist drills with different shank and tip geometries. In this paper, a two-flute, right-cut, straight shank type of solid twist drill is modeled. This is the most commonly used drill for originating holes.

Geometrically a drill is made of (i) a drill body and (ii) a shank. The drill body is the portion responsible for material removal and the part by which the drill is held and driven in a drilling machine is the shank. For the convenience of modeling, the drill body may be segmented into (i) flute and (ii) point geometry. The flute is the cutting portion of the drill extending from shank to the outer corners of the cutting edges. The point of the drill is the portion that facilitates entry of the drill into the work piece and is an extension of the drill body. The drill flute is composed of two parts- the primary (or cutting edge) flute and the secondary (or non-cutting edge) flute [11]. The primary flute is that portion of the drill flute which yields the cutting edge through the intersection of the flute and grinding surfaces. The secondary flute is not as critical as the primary flute for the cutting action. Its shape can be defined in a manner to facilitate effective removal of chips and to provide sufficient strength and rigidity to the drill body. The geometry of the fluted shank of a twist drill is formed by sweeping helically the cross-section of the drill profile across the length of cylindrical fluted portion of

the drill (L). The parameter of sweeping is determined by the helix angle (λ), or the ratio of diameter of cutting end of drill (D_c) to the pitch (P). The fluted surface of a two-flute drill is made up of three surface patches, namely, land (Σ_1), flank (Σ_2) and Face (Σ_3). The point geometry of the twist drill is dependent on the grinding parameters, which include the angle of drill positioning (β_o), cone half angle (δ) and the offset of the apex of the cone (surface of revolution in grinding process) from the drill axis, H_x and H_y.

2.1 Sectional Geometry

The sectional geometry of the fluted shank comprises of a composite curve formed by joining the vertices $V_1,...,V_4$. It has three segments V_1V_2, V_2V_3 and V_3V_4 as shown in Fig. 1. Segment V_1V_2 is a straight line and forms the land, when swept helically. The other two segments are NURBS curves clamped on both the ends, and on sweeping form flank and face, respectively. The control points to design the flank are chosen in such a way that they provide for the body clearance. The geometry of sectional curve depends on various dimensional parameters like diameter of cutting end of drill (D_c), web radius (r_w), width of the land (l); order of NURBS curves (m), weights (w_i) and control points ($\vec{b}_i$) for the flank and face; and inclination angle of the land about axis (γ). Segments V_2V_3 and V_3V_4 are given as curves $\vec{p}_2(s)$ and $\vec{p}_3(s)$, and defined as

$$\vec{p}_j(s) = \frac{\sum_{i=0}^{n} w_i N_{m,m+i}(s)\vec{b}_i}{\sum_{i=0}^{n} w_i N_{m,m+i}(s)}, \qquad j = 2,3. \tag{2.1}$$

where, $N_{1,i}(s) = \delta_i$ such that $\delta_i = 1$ for $s \in [s_{i-1}, s_i)$,

$= 0$, elsewhere

$$N_{m,m+i}(s) = \frac{s - s_i}{s_{m+i-1} - s_i} N_{m-1,m+i-1}(s) + \frac{s_{m+i} - s}{s_{m+i} - s_{i+1}} N_{m-1,m+i}(s) \tag{2.2}$$

Here, N is the shape function and n is the number of control points.

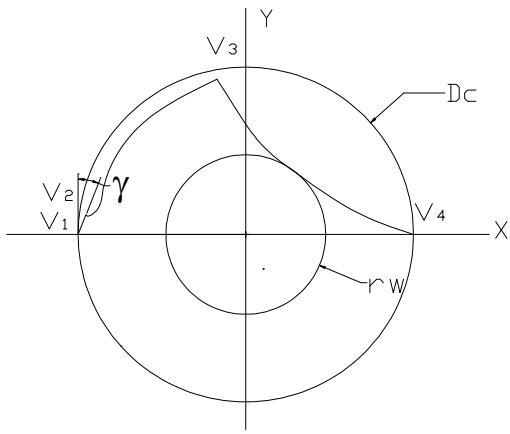

Fig. 1: Sectional geometry of the drill model.

2.2 Flute Geometry

The flute geometry is obtained when the sectional curve is rotated and translated about its axis. It consists of helicoidal surfaces Σ_1, Σ_2 and Σ_3. The sweep matrix is given as:

$$[T_s] = \begin{bmatrix} \cos\phi & \sin\phi & 0 & 0 \\ -\sin\phi & \cos\phi & 0 & 0 \\ 0 & 0 & 1 & 0 \\ 0 & 0 & \frac{P\phi}{2\pi} & 1 \end{bmatrix} \quad (2.3)$$

where $0 \leq \phi \leq \frac{2\pi L}{P}$

The helicoidal surfaces Σ_1 to Σ_3 are formed on the basis of following sweep rules:

Land: $$\Sigma_1 = \vec{p}_1(s).[T_s] = \vec{p}_1(s,\phi) \quad (2.4)$$

Flank: $$\Sigma_2 = \vec{p}_2(s).[T_s] = \vec{p}_2(s,\phi) \quad (2.5)$$

and, Face: $$\Sigma_3 = \vec{p}_3(s).[T_s] = \vec{p}_3(s,\phi) \quad (2.6)$$

where $0 \leq s \leq 1$, and $\vec{p}_i(s)$ is the curve vector having end points V_i and V_{i+1}.

The flute geometry for the remaining part of the drill can be obtained by rotating the respective surfaces by 180^0 about Z-axis. The corresponding surfaces are termed as Σ'_1, Σ'_2 and Σ'_3 respectively.

2.3 Point Geometry

The drill point is made up of as many surface patches as the number of flutes. For a two-flute drill, two surface patches form the drill point. They are labeled as Σ_4 and Σ_5, and are the two lip relief surfaces. The major cutting edges of the drill called as lips are formed by the intersection of the helical surface of a flute with the lip relief surfaces. The edge at the end of the drill is called chisel edge and formed due to the intersection of the lip relief surfaces. The lip relief surface can be planar, cylindrical, conical, helicoidal or of any generic shape. For a conical drill point, the grinding profile is shown in Fig. 2a. Fig. 2b shows the grinding profile for a generic drill point. For the generic drill point, the generatrix of the grinding surface is not a straight line, but rather a NURBS.

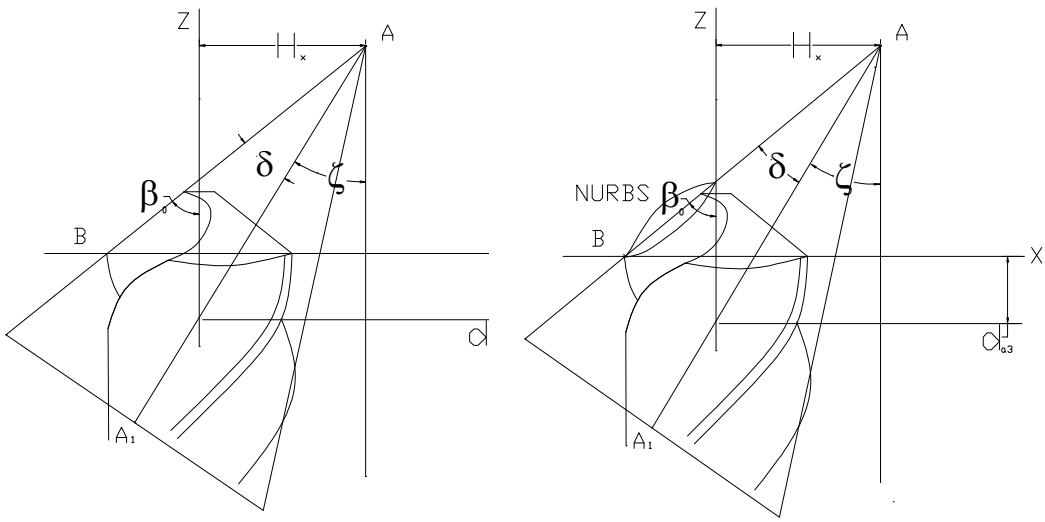

Fig. 2: (a) Conical drill point, (b) Generic drill point.

For the point, the flank Σ_2 is in contact with lip relief surface Σ_4 at the end of the fluted shank. Surface Σ_4 is a segment of a cone of the half angle δ. The apex of the cone is placed at a distance H_x from the drill axis along the x-axis and $-H_y$ along the y-axis from the drill axis, where H_x, H_y are both positive.

Lip relief surface Σ_4 is formed as a surface of revolution by rotating edge AB about the axis AA_1 as shown in Fig. 5. The edge AB is parametrically defined as

$$\vec{e}_{ab}(t) = \left[\left\{ \frac{-D_c}{2} + t\left(H_x + \frac{D_c}{2}\right) \right\} \quad -H_y \quad \frac{t\left(H_x + \frac{D_c}{2}\right)}{\tan\beta_o} \quad 1 \right], \; 0 \le t \le 1 \tag{2.7}$$

Surface Σ_4 is given by: $$\Sigma_4 = \vec{p}_4(t,\varphi) = \vec{e}_{ab}(t).[R_{AA_1}] \tag{2.8}$$

where $[R_{AA_1}]$ is the rotation matrix about axis AA_1 and,

$$[R_{AA_1}] = [T_{y,d_{a_2}}].[T_{z,d_{a_3}}].[R_{y,-\zeta}].[R_{z,\varphi}].[R_{y,-\zeta}]^{-1}.[T_{z,d_{a_3}}]^{-1}.[T_{y,d_{a_2}}]^{-1} \tag{2.9}$$

Matrix $[T_{y,d_{a_2}}]$ is the translation matrix required to displace axis AA_1 along the Y-direction by d_{a_2} so that it intersects with the Z-axis. Thus, here $d_{a_2} = H_y$ as the axis AA_1 is parallel to the ZX plane. Matrix $[T_{z,d_{a_3}}]$ is the translation matrix meant for displacing axis AA_1 along the Z-direction by

$$d_{a_3} = \frac{H_x}{\tan\zeta} - \frac{H_x + \frac{D_c}{2}}{\tan\beta_o} \tag{2.10}$$

so that the axis AA_1 passes through the origin. Matrices $[R_{y,-\zeta}]$ and $[R_{z,\varphi}]$ are rotation matrices about Y and Z-axes by angles $-\zeta$ and φ respectively in the anticlockwise direction. Angle β_o is the angle of drill positioning and is influenced by point angle 2β and can be calculated from the Tab. 1. Angle ζ is given by the relation $$\zeta = \beta_o - \delta \tag{2.11}$$

The parametric equation of the surface Σ_4 is given by the following relations:

$$p_{4X}(t,\varphi) = A(\cos^2\zeta\cos\varphi + \sin^2\zeta) - B(\cos\zeta\sin\zeta\cos\varphi - \cos\zeta\sin\zeta) \tag{2.12}$$

$$p_{4Y}(t,\varphi) = A\cos\zeta\sin\varphi - B\sin\zeta\sin\varphi - d_{a2} \tag{2.13}$$

$$p_{4Z}(t,\varphi) = -A(\cos\zeta\sin\zeta\cos\varphi - \cos\zeta\sin\zeta) + B(\sin^2\zeta\cos\varphi + \cos^2\zeta) - d_{a3} \tag{2.14}$$

where, $A = \left\{ -\frac{D_c}{2} + t(H_x + \frac{D_c}{2}) \right\}$, $B = \left\{ \frac{t(H_x + \frac{D_c}{2})}{\tan\beta_0} + d_{a3} \right\}$, $0 \le t \le 1$

Second lip relief surface Σ_5 is formed by rotating Σ_4 about the axis by an angle of 180^0. For an n-fluted drill, surface patches Σ_{4+j} can be formed by rotating the surface patch Σ_4 about the axis by angles $\left(\frac{2\pi j}{n}\right)^0$ respectively, where $j \to 1...(n-1)$.

Relief angle α (degrees)	Point angle 2β						
	60	70	90	118	140	160	180
	Angle β_0 (degrees)						
6	30	35	45	59	70	79	86
12	30	35	45	58	68	76	80
18	30	35	44	57	66	71	74
24	30	35	44	56	62	66	68

Tab. 1: Approximate values of drill axis angles [23].

2.4 Cutting Lip

The cutting lip is obtained as the intersection of the face with the grinding surface. The curve can be obtained by solving for surface-surface intersection using Timmer's method. Alternatively, the problem can be reduced to finding out the intersection between a curve and a surface and the points of intersection can be obtained using optimization algorithms.

At a point of intersection, $\vec{d_1}|_z = \vec{p_3}'(s,\phi)|_z - \vec{p_4}(t,\varphi) = 0$ (2.15)

where $\vec{p_3}'(s,\phi)|_z$ is the curve traced on $\vec{p_3}'(s,\phi)$ at any z. $\vec{p_3}'(s,\phi)$ is the helicoidal surface given by $\vec{p_3}'(s,\phi) = p'_3(s).[T_s]$ and $p'_3(s)$ is the curve obtained by rotating $p_3(s)$ by 180^0. $\vec{d_1}|_z$ is the minimum distance between the curve and the surface at a chosen value of z.

In this paper, the points of intersection have been obtained using MATLAB optimization algorithms. $\vec{d_1}|_z$ is minimized to obtain the points of intersection.

2.5 Chisel Edge

The chisel edge is obtained as the intersection of Σ_4 and Σ_5. The intersection of the two surfaces can be found out by finding out the points where

$$\vec{d_2} = \vec{p_4}(t,\varphi) - \vec{p_5}(t,\varphi) = 0 \quad (2.16)$$

To simplify the problem, the contour of the surfaces at different values of z are found and points of intersection obtained. This problem can again be solved using optimization technique.

$$\vec{d_2}|_z = \vec{p_4}(t,\varphi)|_z - \vec{p_5}(t,\varphi)|_z = 0 \quad (2.17)$$

The extremities of the chisel edge are evaluated by finding the intersection of $\Sigma_3, \Sigma_4, \Sigma_5$ and $\Sigma'_3, \Sigma_4, \Sigma_5$. The first of these is obtained by solving the equation:

$$d_3^2 = |\vec{p_4}(t,\varphi) - \vec{p_5}(t,\varphi)|^2 + |\vec{p_3}(s,\phi) - \vec{p_4}(t,\varphi)|^2 + |(\vec{p_3}(s,\phi) - \vec{p_5}(t,\varphi)|^2 = 0 \quad (2.18)$$

Similarly, the second. The peak of the chisel edge will lie on the z-axis.

To obtain the generic profiles, a drill was chosen and the coordinates on a section of the fluted part were obtained. They are given in Tab. 2. Using the parameters listed below, the surfaces of sweep and revolution were obtained. The cutting lips and the chisel edge were subsequently obtained using optimization algorithms. The sectional profile, the flute geometry, the conical grinding surfaces and the grinding surfaces with a generic profile are shown in Figs. 3-6 respectively. The cutting lips and the chisel edge are shown in Fig. 7. It can be seen from Fig. 7 (a) and (b) that the cutting lip is curved and the chisel edge has a slightly curved S-shape.

D_c = 14 mm	P = 68.3 mm	r_w = 0.7 mm
L = 131 mm	l = 0.83 mm	$\gamma = 10.9^0$
$\beta_0 = 59^0$	d_{a_2} =2 mm	$\delta = 50^0$

Tab. 2: Drill profile data.

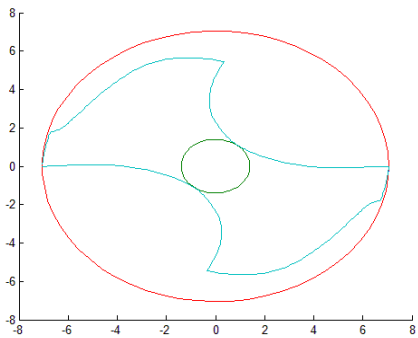

Fig. 3: Sectional profile of the generic model.

Fig. 4: Flute profile of the generic model.

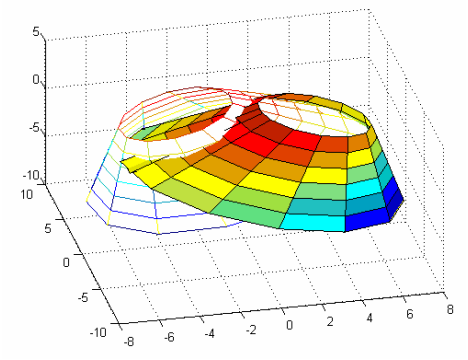

Fig. 5: Conical Grinding surfaces of revolution.

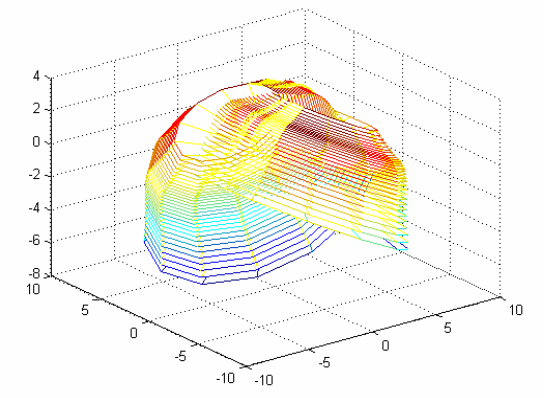

Fig. 6: Grinding cone with a generic profile.

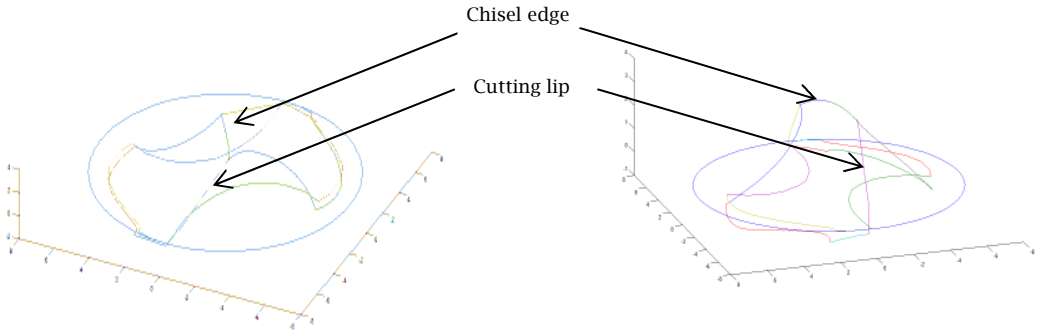

Fig. 7 (a) and (b): Two views of the cutting lips and chisel edge.

3. MECHANISTIC FORCE MODELING

The forces in drilling for the generic geometric model have been calculated based on mechanistic calculations [3-4].

3.1 Cutting Lip Force Model

The points on the cutting lip obtained through surface-curve intersection algorithm are stored in a matrix. The neighboring points are joined by a straight line and treated as cutting elements on the lip. A local coordinate frame is fixed to the centre of each element while the world coordinate frame is fixed to the drill, with the z-axes of the two frames being parallel. The local and world coordinate frames are related as:

$$\hat{e}_{Xw} = \hat{e}_{xl}\cos\psi + \hat{e}_{yl}\sin\psi \tag{3.1}$$

$$\hat{e}_{Yw} = -\hat{e}_{xl}\sin\psi + \hat{e}_{yl}\cos\psi \tag{3.2}$$

where ψ is the angle of revolution of the drill axis and is given by $\psi = \omega.t$, where ω is the angular velocity and t is the time. Using the matrix of the cutting elements, the cutting lip element is defined as a vector $\vec{L}$. The velocity vector is obtained as $\vec{V} = \vec{\omega}\mathrm{x}\vec{r}$, where r is the radius vector of the midpoint of the cutting lip in the world frame. The inclination angle (i) is obtained using the relation

$$\cos(90 + i) = \vec{L}.\vec{V} \tag{3.3}$$

Normal to the face is obtained as the normalized cross-product of the two parameters making the biparametric surface patch:

$$\hat{N} = \frac{\vec{p}_4^{'s} \text{x } \vec{p}_4^{'\phi}}{|\vec{p}_4^{'s} \text{x } \vec{p}_4^{'\phi}|} \tag{3.4}$$

where $\vec{p}_4^{'s}$ and $\vec{p}_4^{'\phi}$ denote the derivatives of $\vec{p}_4^{'}(s,\phi)$ respectively.

Thus normal rake angle is obtained as: $$\cos(\frac{\pi}{2} - \alpha_n) = \hat{N}.(\frac{\vec{V}\text{x}\vec{L}}{|\vec{V}\text{x}\vec{L}|}) \tag{3.5}$$

The chip thickness at the element is given as: $$t_c = \frac{f}{2}\sin k \tag{3.6}$$

where k is the point angle for the cutting element and calculated from the coordinates of the extremities of the element as :

$$k = \tan^{-1}\left(\frac{\Delta X}{\Delta Z}\right) \tag{3.7}$$

Now the magnitude of the elemental Normal $|d\vec{F}_n|$ and Friction force $|d\vec{F}_f|$ are computed from the oblique-cutting model. The mechanistic force equations are

$$|d\vec{F}_n| = K_n.A_c \tag{3.8}$$

$$|d\vec{F}_f| = K_f.A_c \tag{3.9}$$

where, K_n and K_f are the Specific Normal and Friction forces and A_c is the chip load. They can be further expressed in terms of the chip thickness t_c, velocity V and normal rake angle α_n as

$$\ln K_n = a_0 + a_1 \ln t_c + a_2 \ln V + a_3 \ln(1 - \sin\alpha_n) + a_4 \ln t_c \ln V \tag{3.10}$$

$$\ln K_f = b_0 + b_1 \ln t_c + b_2 \ln V + b_3 \ln(1 - \sin\alpha_n) + b_4 \ln t_c \ln V \tag{3.11}$$

where $a_0 ... a_4$ and $b_0 ... b_4$ are constants to be evaluated experimentally.

Assuming the Stabler's rule for the chip flow angle, the normal and friction forces can be used to get the magnitude of the elemental oblique cutting thrust, cutting force and lateral force. They are related as:

$$\begin{bmatrix} |d\vec{F}_{th}| \\ |d\vec{F}_{cut}| \\ |d\vec{F}_{lat}| \end{bmatrix} = \begin{bmatrix} \cos i \cos\alpha_n & -\sin\alpha_n \\ \sin^2 i + \cos^2 i \sin\alpha_n & \cos i \cos\alpha_n \\ \cos i \sin i \cos\alpha_n - \sin i \cos i & \sin i \cos\alpha_n \end{bmatrix} \begin{bmatrix} |d\vec{F}_n| \\ |d\vec{F}_f| \end{bmatrix} \tag{3.12}$$

The elemental cutting force vector is against the direction of the cutting velocity vector in direction. The direction of the elemental thrust force vector is cross product of the unit velocity and lip vectors given by $\frac{\vec{V}\text{x}\vec{L}}{|\vec{V}\text{x}\vec{L}|}$. The elemental lateral force vector is perpendicular to the cutting force and the thrust force and its direction is given by $\frac{-d\vec{F}_{cut}\text{x } d\vec{F}_{th}}{|d\vec{F}_{cut}\text{x } d\vec{F}_{th}|}$.

Using the above, the radial forces, the thrust force and the torque can be calculated. The thrust force is the sum of the z-components of the three forces given by

$$|d\vec{F}_{zl}| = |d\vec{F}_{th,z} + d\vec{F}_{cut,z} + d\vec{F}_{lat,z}| \tag{3.13}$$

The torque is given by: $$|d\vec{M}_{zl}| = |\vec{r}\,||d\vec{F}_{cut}| \tag{3.14}$$

The magnitudes of the total drilling thrust $|\vec{F}_{Zw}|$ and torque $|\vec{M}_{Zw}|$ are obtained by summing the forces at all the cutting elements engaged in the cut on each lip of the drill.

3.2 Chisel Edge Force Model

Having modeled the forces on the cutting lip, the forces on the chisel edge are modeled. In a region around the centre of the drill called the indentation zone, material removal is by extrusion. The radius of the indentation zone R_a is given as

$$R_a = \frac{f_r}{2\pi \tan \gamma_s} \tag{3.15}$$

where f_r is the feed per revolution of the drill and γ_s is the static clearance angle given by

$$\gamma_s = \frac{\pi}{2} - \eta \tag{3.16}$$

and η is half the wedge angle of the chisel edge at the centre of the drill point. For the conical surface of revolution, η is given by

$$\eta = \tan^{-1}((H_x^2 + {d_{a2}}^2)^{1/2}.\tan B_0 / H_x) \tag{3.17}$$

The thrust Th_{ind} and torque To_{ind} due to the indentation process at the chisel edge are given as:

$$Th_{ind} = \frac{4K(1+\varepsilon) f_r R_a \sin \alpha_{n,ch}}{\cos \alpha_{n,ch} - \sin(\alpha_{n,ch} - \varepsilon)} \tag{3.18}$$

$$To_{ind} = \frac{2K(1+\varepsilon) f_r R_a^2 \cos \alpha_{n,ch}}{\cos \alpha_{n,ch} - \sin(\alpha_{n,ch} - \varepsilon)} \tag{3.19}$$

where, $\alpha_{n,ch}$ is the static normal rake angle at the chisel edge and equal to half the included angle of the wedge. It is equal to η at the centre of the drill point. The height of indentation is $f_r/2$ for two-fluted drill, and ε is the solution of the slip line given by

$$2\alpha_{n,ch} = \varepsilon + \cos^{-1}\{\tan(\frac{\pi}{4} - \frac{\varepsilon}{2})\} \tag{3.20}$$

The secondary cutting edge forces are calculated in a similar manner as the cutting lips. The chip thickness here is $f_r/2$ if the number of lips is two. Since the tangential velocity at the secondary cutting edges is small, the feed velocity needs to be included. The resultant velocity will now be the vector sum of the tangential velocity and the feed velocity. The static normal rake angle $\alpha_{n,ch}$ is defined with respect to the tangential velocity vector only. The normal rake angle in an oblique cutting process is defined with respect to the normal to the finished surface which also the direction of the resultant velocity vector. The dynamic normal rake angle is equal to the sum of the static normal rake angle and the feed angle ϕ_f, and is given by

$$\alpha_{d,ch} = \alpha_{n,ch} + \phi_f \text{ , where } \phi_f = \tan^{-1}(\frac{f_r}{2\pi r}) \tag{3.21}$$

The dynamic rake angle is used to compute the Specific Normal and Friction forces and the static normal rake angle is used to resolve these forces into the drilling thrust and torque equations.

3.3 Application of the Force Model

The mathematical force model developed requires the evaluation of constants $a_0,\ldots,a_4$ and $b_0,\ldots,b_4$ to calculate the forces. Using the results of the calibration tests with a conical drill [3] for the tool material being TiN coated High Speed steel and work piece material being 1018 steel, the Eqns. (3.10) and (3.11) can be written as

$$\ln K_n = 7.642 - 0.153 \ln t_c - 0.143 \ln V + 0.704 \ln(1 - \sin \alpha_n) + 0.086 \ln t_c \ln V \tag{3.22}$$

$$\ln K_f = 7.267 - 0.262 \ln t_c - 0.067 \ln V + 0.407 \ln(1 - \sin \alpha_n) + 0.081 \ln t_c \ln V \tag{3.23}$$

The data are fed into MATLAB codes and the thrust and torque are evaluated using the grinding parameters for conical grinding (Figs. 8, 9). To observe the chisel edge and cutting lip forces separately, in order to be able to compare them, a pilot hole is used, whose diameter is exactly equal to the web-diameter of the drill.

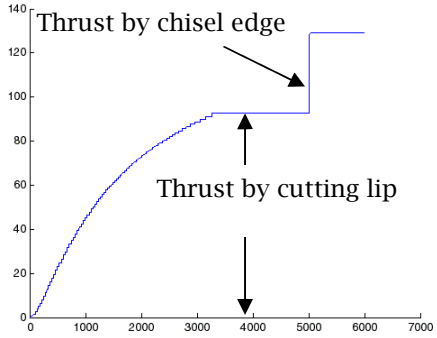

Fig. 8: Thrust (N) vs. time (ms).

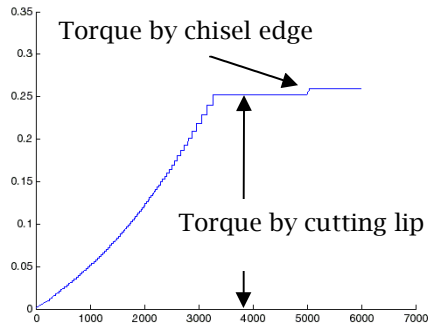

Fig. 9: Torque (N-m) vs. time (ms).

4. SUMMARY AND CONCLUSIONS

- The geometry of a drill point is modeled using NURBS, which gives the freedom to model a generic drill profile. The cutting edges obtained here are curved in space and not straight, and related to the grinding parameters. This helps modify the grinding parameters to obtain the desired drill point profile.
- Optimization Algorithm has been employed to obtain the surface-surface intersection points. The cutting lip is obtained as the intersection of a sweep surface and a surface of revolution, while the chisel edge is obtained as the intersection of two surfaces of revolution. The neighboring points are connected to have the oblique cutting elements and the cutting angles are evaluated for the individual elements.
- The mechanistic model is subsequently applied to calculate the forces for each element which are further resolved and added to give the total thrust and torque by the drill.

In summary, the proposed methodology gives us a freedom to model any kind of drill point profile and calculate the thrust and torque mechanistically.

The research is to be further continued to give the optimum drill point geometry for minimum thrust and torque where the cutting lips and the chisel can be given a generic shape using NURBS.

REFERENCES

[1] Armarego, E. J. A.; Cheng, C. Y.: Drilling with Flat Rake Face and Conventional Twist Drills. I- Theoretical Investigations and II- Experimental Investigations, International Journal of Machine Tool Design and Research, 12, 1972, 17-54.

[2] Armarego, E. J. A.; Wright, J. D.: Predictive Models for Drilling Thrust and Torque – A Comparison of Three Flank Configurations, Annals of the CIRP, 33(1), 1984, 5-10.

[3] Chandrasekharan, V.; Kapoor, S. G.; DeVor, R. E.: A Mechanistic Model to Predict the Cutting Forces in Drilling: With Application to Fiber Reinforced Composite Materials, ASME Journal of Engineering for Industry, 117, 1995, 559–570.

[4] Chandrasekharan, V.; Kapoor, S. G.; DeVor, R. E.: Mechanistic Model to Predict the Cutting Force System for Arbitrary Drill Point Geometry, Journal of Manufacturing Science and Engineering, 120, 1998, 563–570.

[5] Cho, N. W.; Kim, N. K.; Kim, Y.; Kang, S. H.: An Evolutionary Method for General Surface-Surface Intersection Problems, Computers in Industry and Engineering, 33(3-4), 1997, 573-576.

[6] Fugelso, M. A.: Conical Flank Twist Drill Points, International Journal of Machine Tools and Manufacture, 30(2), 1990, 291-295.

[7] Fugelso, M. A.: A Standard Conical Point Drill Grinding Machine, International Journal of Machine Tools and Manufacture, 41, 2001,915-922.

[8] Fuh, K. H.; Chen, W. C.: Cutting Performance of Thick Web Drills with Curved Primary Cutting Edges, International Journal of Machine Tools and Manufacture, 35(7), 1995, 975-991.

[9] Fujii, S.; DeVries, D. F.; Wu, S. M.: An Analysis of Drill Geometry for Optimum Drill Design by Computer – Part I: Drill Geometry Analysis, Part II: Computer Aided Design, ASME Journal of Engineering for Industry, 92(3), 1970, 647-666.
[10] Fujii, S.; DeVries, D. F.; Wu, S. M.: Analysis of the Chisel Edge and Effect of the d-theta Relationship on Drill Point Geometry, ASME Journal of Engineering for Industry, 93(4), 1971, 1093-1105.
[11] Galloway, D. F.: Some Experiments on the Influence of Various Factors on Drill Performance, Transactions of the ASME, 79, 1956, 191-231.
[12] Lin C.; Kang, S. K.; Ehmann, K. F.: Helical Micro-drill Point Design and Grinding, ASME Journal of Engineering for Industry, 117, 1995, 277-287.
[13] Paul, A.; Kapoor, S. G.; DeVor, R. E.: A Chisel Edge Model for Arbitrary Drill Point Geometry, Journal of Manufacturing Science and Engineering, 127, 2005, 23-32.
[14] Paul, A.; Kapoor, S. G.; DeVor, R. E.: Chisel Edge and Cutting Lip Shape Optimization for Improved Twist Drill Point Design, International Journal of Machine Tools and Manufacture, 45, 2005, 421-431.
[15] Rubeinstein, C.: The Torque and Thrust Force in Twist Drilling. I- Theory and II- Comparison of Experimental Observations and Deductions from Theory, International Journal of Machine Tools and Manufacture, 31 (4), 1991, 481-504.
[16] Shi, H. M.; Zhang, H. S.; Xiong, L. S.: A Study on Curved Edge Drills, ASME Journal of Engineering for Industry, 116, 1994, 267–273.
[17] Stephenson, D. A.; Agapiou, J. S.: Calculation of Main Cutting Edge Forces and Torque for Drills With Arbitrary Point Geometries, International Journal of Machine Tools and Manufacture, 32, 1992, 521–538.
[18] Tandon, P.; Gupta, P.; Dhande, S. G.: Geometric Modeling of Fluted Cutters, Journal of Computing and Information Science in Engineering, 8, 2008, 1-15.
[19] Tsai, W. D.; Wu, S. M.: A Mathematical Model for Drill Point Design and Grinding, ASME Journal of Engineering for Industry, 101, 1979, 330-340.
[20] Wang, J.; Zhang, Q.: A study of high-performance plane rake faced twist drills. Part II: Predictive force models, International Journal of Machine Tools Manufacture, 48, 2008, 1286– 1295.
[21] Watson, A. R.: Drilling Model for Cutting Lip and Chisel Edge and Comparison of Experimental and Predicted Results. I- Initial Cutting Lip Model, II- Revised Cutting Lip Model, III- Drilling Model for Chisel Edge, IV- Drilling Tests to Determine Chisel Edge Contribution to Thrust and Torque, International Journal of Machine Tool Design and Research, 25(4), 1985, 347-404.
[22] Xiong, L.; Fang, N.; Shi, H.: A New Methodology for Designing a Curve-edged Twist Drill with an Arbitrarily Given Distribution of the Cutting Angles along the Tool Cutting Edge, International Journal of Machine Tools & Manufacture, 49, 2009, 667-677.
[23] Popov, S.; Dibner, L.; Kamenkovich, A.: Sharpening of Cutting Tools, Mir Publishers, Moscow, 1988.